Tunnel-vision on economic linear propulsion?

Veltman, André; van der Hulst, Paul; Jonker, Marco; Polinder, Henk

DOI
10.1109/LDIA.2019.8771014

Publication date
2019

Document Version
Final published version

Published in
12th International Symposium on Linear Drives for Industry Applications (LDIA 2019)

Tunnel-Vision on Economic Linear Propulsion?

André Veltman[1], Paul van der Hulst[1], Marco Jonker[2] and Henk Polinder[3]
1 Piak Electronic Design B.V., the Netherlands
2 Engie Electroproject B.V., the Netherlands
3 Delft University of Technology, the Netherlands

***Abstract*—Serious initiatives for high speed transport of vehicles/pods/capsules through evacuated tubes were presented in recent years. Most suggest magnetic levitation and linear motors of long-stator design, assuming passive pods. This paper takes a the different approach, yielding minimal energy use per distance per passenger and lowest initial cost. An active pod (short-stator) on wheels with an on-board battery, able to build up speed and regenerate effectively using an inexpensive passive track is proposed. In the stations, power is received from active track-coils to charge the on-board battery. Permanent magnet (PM) track sections enable thrust to speed-up and slow-down. A relatively small rotating induction motor on the wheels enables efficient coasting. Speeding up and slowing down with a linear motor at constant power is effective in terms of component utilization. A mere 100 W/kg (common in present commercial full electric cars) is sufficient to travel long distance at high speed on record low energy consumption (<10 Wh/km per passenger).**

***Index Terms*—Linear motors, LSM, doubly-fed, high speed, low drag**

I. Introduction

In many science fiction stories and present hyperloop designs magnetic levitation is presented as a must. However physical facts suggest otherwise, wheels show the lowest-drag of all options. Which is the most favorable linear motor type: long- or short-stator? Long-stator type linear motors are used in Transrapid, SCmaglev [5], Hyperloop-one and launching rollercoasters [7]. Fortunately our experience with multi megawatt linear motors in roller coasters seems also applicable to long distance fast transport in evacuated tubes.

For high acceleration it is beneficial to be 'pushed' by an active shore-system with high power: a long-stator design. Roller-coasters and test-sites that combine high speed with short tubes need such. However, systems with low drag do not need high power to coast at any constant speed. The coasting-power and energy is sufficiently low to be supplied from an on-board battery via an inverter to an on-board pod-coil: a short-stator design. A much simpler and more economic track results in this case.

II. Units and Drag

Energy consumption per unit distance and effective drag-force are essentially the same thing. As energy consumption is expressed in amount of energy (fuel) per unit distance, energy (Nm) per distance (m) boils down to an effective drag expressed in newtons. A car doing 15 km/liter then results, using table I, in a (fuel)force of 2.5 kN. Regarding the combustion engine's efficiency of say 30%, a mechanical drag of 844 N makes sense. Table I shows how used units can be translated into force or the cross-sectional area of a 'rod' of fuel being burnt.

TABLE I
Units of efficiency in transport

unit	equivalent
MJ/km	1000 N
Wh/km	3.6 N
MJ/(kg.km)	1 N/kg = 0.102 g
W/(km/h)	3.6 N
liter/100km	0.01 mm^2
liter/100km (fuel 40MJ/liter)	400 N
km/liter(fuel 40MJ/liter)	1/(40kN)
mile/Gallon	0.425 km/liter

Relative units, useful for comparing different means of transport are the force-related maximum acceleration $a_{\max}$ (m/s^2) and the specific power p_{spec} (W/kg) that defines the highest acceleration possible at a given speed. Relative drag or 'drag coeficient' D/L is defined as the unit drag per unit lift. Terms 'vehicle', 'pod' and 'capsule' are used as synonyms.

III. Dragging on

In cars, trains and planes the dominant drag-component at mechanical speed v_{m} (m/s) originates from displacing air which can be approximated by $\mathcal{F}_{\text{air}}(v_{\text{m}})$ in (1). The build up of the total drag of a capsule with mass m_{pod}, gravitational acceleration g, frontal area A_{front} by suspension induced drag $\mathcal{F}_{\text{susp}}$ and air friction $\mathcal{F}_{\text{air}}$ is given in (1). The blockage ratio is part of the aerodynamic shape-constant c_{w}, ρ is the density of air or fluid:

$$\mathcal{F}_{\text{drag}} = \underbrace{m_{\text{pod}} g C_{\text{susp}}}_{\mathcal{F}_{\text{susp}}} + \underbrace{\frac{1}{2}\rho\, A_{\text{front}} c_{\text{w}}\, v_{\text{m}}^2}_{\mathcal{F}_{\text{air}}} \tag{1}$$

Friction-free movement, even in an evacuated tube, is not possible.

A. Drag-Strategy

When efficient traveling at high velocity is the goal, (1) suggests that it makes sense to reduce the air's density ρ, either by flying at high altitude, or by evacuating a tube to drive in. Fig. 1 shows two Concorde points, one for super-sonic and one for sub-sonic flight. The purple, blue and green lines in the log-log plot represent the quadratic behavior between speed and drag, the benefit of reduced pressure on drag is obvious. The TGV record of 574.8 km/h is close to the purple ICE line, indicating comparable weight and effective frontal area. The

978-1-5386-5804-8/19/$31.00

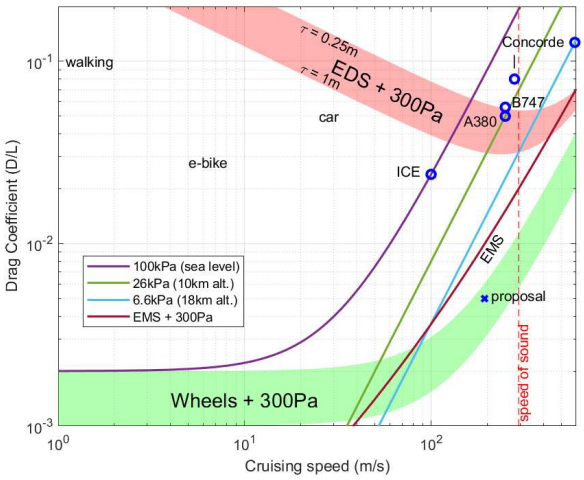

Fig. 1. Mechanical drag per weight versus speed, based on data from [3] with air-drag added, here presented on logaritmic scales to clearify the quadratic behavior of $\mathcal{F}_{\text{air}}$ and compare proposed linear drive on wheels.

green area represents the proposed system on wheels, rolling in air pressure equivalent to flying at about 30 km altitude.

B. Electro Dynamic Suspension (EDS)

EDS as described in [3] is based on the repelling force between on-board magnets with pole-pitch τ (m) and induced currents in a conducting sheet or coils in the track. EDS's drag is approached by a constant current in a conducting sheet with skin-effect, implying a drag-force reducing with the square root of the speed: $C_{\text{susp}}(\text{EDS}) \approx \frac{C_{\text{eds}}}{\sqrt{v_{\text{m}}}}$ in (1). EDS is used in SCMaglev and Hyperloop-one as shown as the red area bounded by two pole-pitch values in Fig. 1. This graph shows that EDS drag is so high that only at speeds above 200 m/s EDS-drag becomes comparable to that of a commercial aircraft at 10 km altitude, but still always higher than the ICE train in air at sealevel at 100 m/s.

EDS has high drag, but also needs to plow through the high-loss low-speed region before levitation starts (SCmaglev rolls on wheels for $v_{\text{m}} < 100$ km/h).

C. Electro Magnetic Suspension (EMS)

EMS as used in Transrapid, is based on attractive forces and requires active high bandwidth control and induces speed dependent eddy currents in the track-laminations causing drag that increases with speed and speed squared: $C_{\text{susp}}(\text{EMS}) \approx C_{\text{ems1}} v_{\text{m}} + C_{\text{ems2}} v_{\text{m}}^2$ in (1). In Transrapid the air-drag dominates the EMS-drag by far.

EMS with bias-permanent magnets and coils, although it needs stabilizing control, will be much preferred over EDS at low speeds. However some losses in the huge laminated levitation 'rail' will be generated in the exposed section. Core-losses in laminated magnetic steel are well described in [6], with the use of which is estimated that the EMS-drag is comparable but likely slightly higher than wheels. Basic principles imply that for the same core-material-type used, the total core-loss is proportional to the vehicle mass, speed squared and inversely proportional to the height (thickness) of the laminated track.

An EMS laminated track can be configured into a long-stator LSM with limited thrust of about 10...15 % of the levitation force.

TABLE II
RELATIVE DRAG

Type, speed(km/h)	*Example*	*W/kg*	*D/L (%)*	*kN/pass*
aircraft (800)	A380	≈250	5	1.3...3
car (100)	Toyota Prius	72	6	0.2...0.8
e-car (100)	Tesla (200 Wh/km)	174	5	0.2...0.8
TransRapid (430)		58	3.4	0.21
ICE (320)		18	2.4	0.13
train (140)	Intercity	15	0.4	0.035...0.1
e-bike (20)	(7.7 Wh/km)	3	2.8	0.028
bicycle (20)	(mech...food)	2	2...8	0.03...0.12
walking (5)	(mech...food)	2	8...33	0.08...0.3
wheel+track (any)	in vacuum	-	0.1...0.2	-
proposal (700)	air: 300 Pa	100	0.5	0.018

D. Wheels on track

Rolling friction of hard wheels is near constant and low at all speeds: $C_{\text{susp}}(\text{wheels}) \approx C_{\text{rol}}$ in (1). The statement of Hyperloop-one team [4]: "...However fast wheels can go, by definition it is just not fast enough." is debatable in our opinion, since TGV trains drive on wheels with a record speed of 574.8 km/h in 2007, running over 19 MW of a catenary with a train weighing $265{\cdot}10^3$ kg, ($p_{\text{spec}} = 72$ W/kg, $D/L = 0.0458$).

A turbine driven car drove a record speed of 1227 km/h on pressed aluminum wheels. Having wheels to carry the weight of the vehicle and a linear motor for acceleration and deceleration as proposed in this paper, will prevent wheel-slip and minimize wheel-wear and maintenance.

A beneficial side-effect of choosing wheels is the ease of implementing dampening suspension, lateral guiding, available track-switching techniques and billions of vehicle kilometers of experience.

In [3] is mentioned that wheels always win from EDS in terms of lowest-drag. Adding EDS that is over ten times more lossy than wheels, even at speeds of 200 m/s seems not a 'green' choice. We are the opinion that very low air-drag in an evacuated tube should not be spoiled by introducing lossy levitation systems. EMS, an attractive counterpart, is still an option, but there is a huge difference in initial cost.

E. Threshold speed

Fig. 1 shows that high speed train ICE on wheels, has the lowest drag of all blue circles, even at atmospheric pressure. Lowering the pressure get's us to the green range. An important boundary from (1) is the ρ value where $\mathcal{F}_{\text{air}}$ equals

$\mathcal{F}_{\text{susp}}$. Assuming $m_{\text{pod}} = 10000\,\text{kg}$ and $c_{\text{w}}\,A_{\text{front}} \approx 3\ \text{m}^2$ this boundary results from $\mathcal{F}_{\text{air}} \leq 0.002\,m_{\text{pod}}\,g$:

$$\rho \leq \frac{0.004\,m_{\text{pod}}\,g}{v_{\text{m}}^2\,c_{\text{w}}\,A_{\text{front}}} \approx 0.0035\ [\text{kg/m}^3] \tag{2}$$

Equation (2) implies that at 194 m/s (700 km/h) the air-density in the tube should be about 0.3 % of the normal density, to not-dominate: air-pressure $\leq$ 300 Pa. To simplify further estimations, $D/L = 0.005$ will be assumed, adding 25 % for conversion efficiencies and unexpected, as indicated by the 'proposed' marker in Fig. 1.

IV. Multi-Mode Linear Motor on Wheels

Our suggested design as sketched in Figs.2,3,4, performs fast-charging during boarding and de-boarding, gentle acceleration (during a few minutes) with constant power to a final speed (e.g. 700 km/h), steady coasting for most of the time followed by a regenerative deceleration to the destination station. Most losses are due to drag since kinetic energy is largely regenerated. Commercially available batteries (red unit) and power converters (yellow units) are able to do all this when using a new multi-mode linear motor that consists of an active pod with a coil-assembly (short-stator, iron-less) like a 'fin' along its length that magnetically interacts with a number of different track-type counterparts as shown in Figs. 3 and 4. An LDFM (linear doubly-fed machine) section at the stations charges the on-board batteries, an LSM (linear synchronous machine) section with magnets on the track enables serious acceleration. A rotating induction machine is preferred for low-power coasting (green IM in Fig. 2) and can also be used for return or back-up in case of main-drive failure or vacuum loss.

A pod's weight of 357 kg/pass is proposed, yielding a vehicle of 10000 kg carrying 28 passengers (Airbus A380 specifications: full: 730 kg/pass, no-fuel: 300 kg/pass).

V. Track section types

Four possible thrust $\mathcal{F}$ producing track-types based on magnetic interaction with the pod-coil are shown in Fig. 4. Tangential stress σ indicates a rough estimate of an achievable thrust per unit stator surface.

A. Linear Doubly Fed Machine (LDFM), $\sigma < 40kPa$

Active track with shore-coils fed in parallel by one or more inverters. High power can be extracted by the pod for charging, both during standstill and during acceleration (see Fig. 5). The pod's velocity v_{m} equals the difference between wave-velocities in the shore-coil and pod-coil. The pod's speed v_{m} is positive when going forward, then $v_{\text{podcoil}} = v_{\text{m}} - v_{\text{shorecoil}}$ results. Simultanious charging and controlled acceleration occurs for negative v_{podcoil}.

The mechanical thrust $\mathcal{F}$ (N) is produced by linked flux Ψ_{stator} and pod-coil's amp-turns ni. The mechanical power delivered to the pod equals the power from both active coils:

$$P_{\text{m}} = \mathcal{F}\,(v_{\text{shorecoil}} + v_{\text{podcoil}}) \tag{3}$$

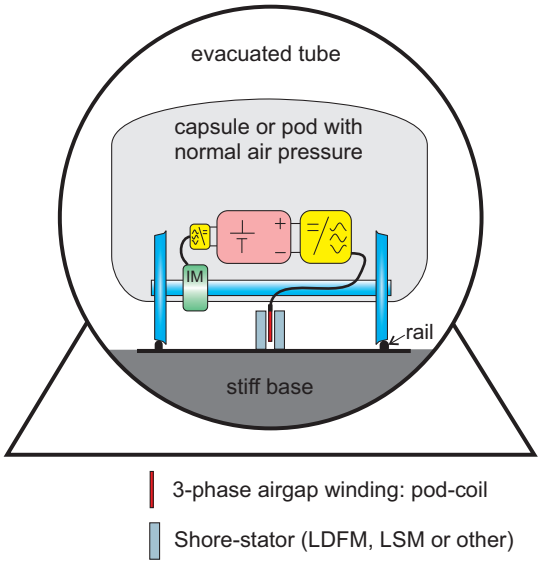

Fig. 2. Sketch of pod on wheels from the rear with linear motor an a speed-keeper motor. The different shore-stator types are sketched in figures 3 and 4.

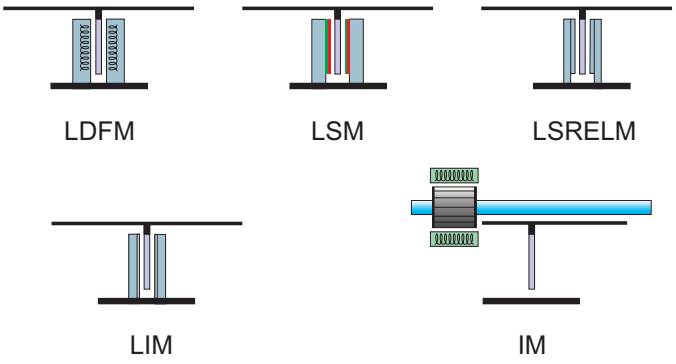

Fig. 3. Close up of shore-stator types, view from rear. (part of Fig. 2).

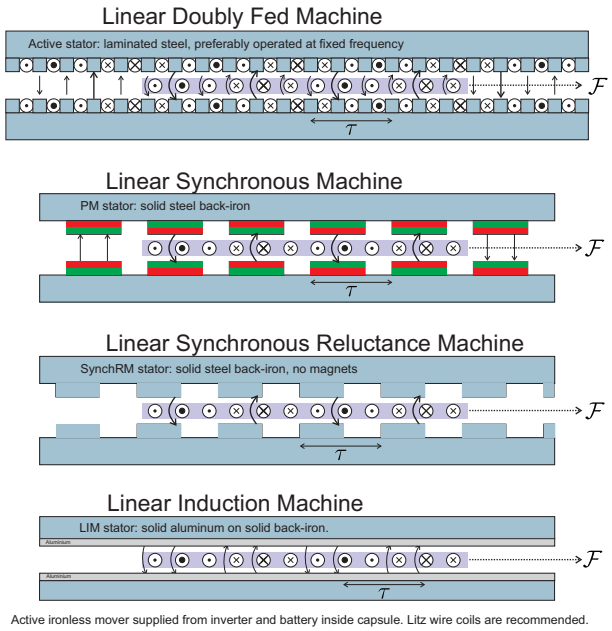

Fig. 4. Multi mode linear machine with moving pod-coil fed from on-board inverter with pole-pitch τ, top view. (part of Fig. 2)

The power P_{shore} delivered by the shore-coils and the power P_{pod} by the pod can each be either positive or negative:

$$P_{\text{shore}} = \mathcal{F}\, v_{\text{shorecoil}} \tag{4}$$

$$P_{\text{pod}} = \mathcal{F}\, v_{\text{podcoil}} \tag{5}$$

As (5) shows, power-transfer is not possible without generating thrust, hence a 'parking brake' is required in the stations to keep the pod in place and $P_{\text{m}} = 0$ to allow for maximum power transfer from shore to pod: fast-charge the on-board battery while $P_{\text{pod}} = -P_{\text{shore}}$.

In Fig. 5 possible connections of the shore coils are shown. Exciting them with a fixed frequency makes efficient soft-switching 6-pulse modulation possible (voltage control). The pod realizes field oriented current-control (FOC). Driving the shore coils in parallel with one ore more inverters mimimizes leakage inductance and enhances power-factor in that way. In the station, only inverters driving coils covered by (part of) a pod-coil need to be energized.

In long distance systems with moderate power levels, active shore-coils on fixed frequency in just the stations will suffice. In systems with high specific power, a variable shore-coil frequency is beneficial to maintain a near constant large $P_{\text{shore}}/P_{\text{pod}}$ ratio during an aggressive launch. The pod's power rating stays moderate and light-weight with perfect FOC.

B. Linear Synchronous Motor (LSM), $\sigma < 40kPa$

Passive track with PM (permanent magnets) fixed to a solid back-iron. Ψ_{stator} selectable by local magnet size and number. High efficiency, suitable for launching [7].

C. Linear Synchr. Reluctance Machine (LSRELM), $\sigma < 20kPa$

Passive track having high permeability material with periodic inductance variations like a solid-iron-rack. Low efficiency due to iron-losses and low power factor, speed-keeping ok.

D. Linear Induction Motor (LIM), $\sigma < 10kPa$

Aluminum plates or ladder structures on solid back-iron. Entry+exit effects and significant slip, speed-keeping ok.

E. Rotating Induction Motor (IM)

Just straight rails, suited for high speed rolling. Pod-coil is not used. Only about 10 % of the acceleration thrust is needed for speed-keeping. By 'rolling up' the LIM, an ordinary rotating IM without end-effects results. A relatively small induction motor can keep the speed (see table IV) with low controllable iron losses whereas in a fast spinning PM motor's iron-losses cannot be controlled.

VI. Constant Power operation

The pod-coil has a ceiling for allowable heating. Heating is caused by current and current produces thrust, hence the pod-coil-design will limit thrust. The on-board inverter is limited in both current and voltage, while the batteries have a discharge-current limit, which implies a power limit. Controlling the system such that the battery power remains almost constant during acceleration to cruising speed is beneficial because

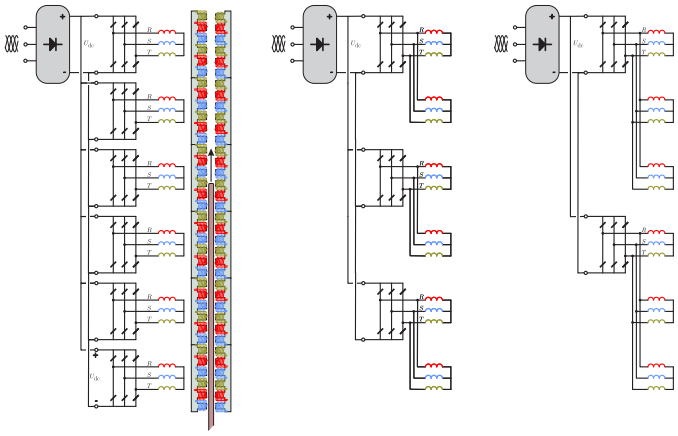

Fig. 5. Shore-coil build up. Left: all pole-pairs with individual 3-phase inverter. Middle: two pole-pairs per converter. Right: three pole-pairs per inverter. In a similar way any number of pole-pairs can be connected to one inverter. Per pole-pair the rating is around 15 kVA.

the system's weakest link (battery) is stressed the least. At low speed the thrust is limited up to the point where the power limit takes over. During constant-power launch thrust lowers when velocity rises (see Fig. 7). The outcome of an extensive derivation, based on newton's laws and ignoring all drag, yields the analytical descriptions in table III: speed and acceleration versus time t and position x .

TABLE III
Launching modes

	constant acceleration	**constant power**
$\frac{p}{m_{\text{pod}}}$ (W/kg)	$p_{\text{spec}} = \frac{v_{\text{ref}}^3}{2x}$	$p_{\text{spec}} = \frac{v_{\text{ref}}^3}{3x}$
$v(t)$ (m/s)	$a\,t$	$\sqrt{2(t-t_0)p_{\text{spec}} + v_0^2}$
$a(t)$ (m/s^2)	$a = \frac{p_{\text{spec}}}{v_{\text{ref}}}$	$\sqrt{\frac{p_{\text{spec}}}{2(t-t_0)}}$
$v(x)$ (m/s)	$(2a\,x)^{\frac{1}{2}}$	$(3p_{\text{spec}}\,x)^{\frac{1}{3}}$
$a(x)$ (m/s^2)	$a = \frac{p_{\text{spec}}}{v_{\text{ref}}}$	$(p_{\text{spec}})^{\frac{2}{3}}\,(3x)^{-\frac{1}{3}}$

The main advantage of constant-power launch is the lower required peak power to reach v_{ref} at the same distance x. A constant power launch is most advantageous when the coupled flux (number of magnets and/or thickness of magnets) is reduced with speed. If flux level Ψ_{stator} is distributed along the track according the lower graph in Fig. 6, the on-board converter can operate under constant current while the flux induces constant voltage and the frequency rises with speed. All graphs start at initial acceleration of 1.5 m/s^2, the red line in the lower graph of Fig. 6 reaches v_{ref} at $x = 24.5$ km.

A. Track consequences

Consider that the forces in the electromagnetic and mechanical domain are:

$$\mathcal{F}(x) = \Psi_{\text{stator}}(x)\, ni = m_{\text{pod}}\, a(x) \tag{6}$$

where x is itself an unknown function in time $x(t)$. This equation describes a stator with length l, which is operated

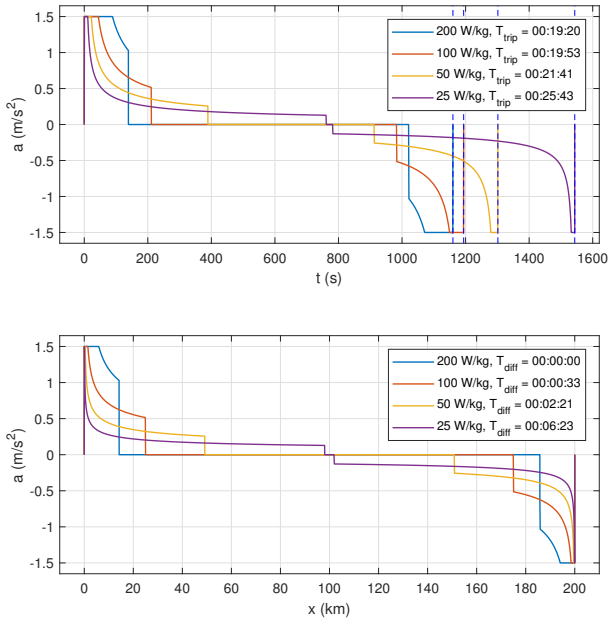

Fig. 6. Short example trip of 200 km to show time (top) and position (bottom) functions with neglected friction for various specific power levels p_{spec}.

with *constant* ni. Table III shows that acceleration $a(t)$ is quite different for the different modes. Power need is lower for constant-power mode, but what about LSM track-cost? Let's try to calculate the total amount of magnets required on the track without presuming any given $a(t)$. After proper integration of (7) over the whole acceleration interval, the total amount of magnet flux in the track Ψ_{total} results in (8).

$$\Psi_{\text{total}} = \int_0^{x_{\text{final}}} \frac{\Psi_{\text{stator}}(x)}{l} \mathrm{d}x \tag{7}$$

$$\Psi_{\text{total}} = \frac{\frac{1}{2} m_{\text{pod}}\, v_{\text{final}}^2}{l\, ni} \tag{8}$$

From (8) can be concluded that the amount of required magnet-flux is proportional to the final kinetic energy and inversely proportional to the length of the pod-coil times the amp-turns ni. No dependency on how slow or fast one wants to accelerate, only assuming that AC-current in the pod-coil is of constant amplitude and correctly oriented to the coupled flux.

VII. On-board energy

A. Maximum speed

The specific energy density of a Lithium Polymer (LiPo) battery is about $W_{\text{Sbat}} = 0.72$ MJ/kg (200 Wh/kg). The kinetic energy required for a launch is $\frac{1}{2} m_{\text{pod}} v_{\text{m}}^2$. The maximum speed v_{max} without drag can now be expressed as a function of battery-weight fraction $k_{\text{bat}} = \frac{m_{\text{bat}}}{m_{\text{pod}}}$:

$$v_{\text{max}} = \sqrt{2 W_{\text{Sbat}} k_{\text{bat}}} \tag{9}$$

Equation (9) reveals that with $k_{\text{bat}} = 10\,\%$, a maximum speed of 379 m/s (1366 km/h) can be reached, assuming no friction and no-loss system components. This is twice the goal speed of 700 km/h and four times the energy.

B. Maximum range

Since most of the energy used for acceleration can be recovered during deceleration, only drag is regarded at this point. The total energy (work) W_{d} lost to drag during the trip with length Δx can be calculated from the available battery energy $W_{\text{bat}} = m_{\text{bat}} W_{\text{Sbat}}$, using g= 9.81 N/kg according:

$$W_{\text{d}} = \underbrace{C_{\text{susp}}\, m_{\text{pod}}\, g}_{\text{(N)}} \underbrace{\Delta x}_{\text{(m)}}$$

$$\frac{W_{\text{d}}}{m_{\text{pod}}} = \underbrace{g\, C_{\text{susp}}\, \Delta x}_{\text{(J/kg)}}$$

$$\Delta x = k_{\text{bat}} \frac{W_{\text{Sbat}}}{g\, C_{\text{susp}}} \tag{10}$$

A range of 147 km results from each percentage point of battery weight according (10). For an example range of 700 km, only $k_{\text{bat}} > 0.05$ is needed when assuming perfect regeneration. A Tesla car with $k_{\text{bat}} \approx 0.25$ has a range of 'only' 500 km due to the normal atmospheric drag. The suggested pod on wheels and 300 Pa air-pressure would have a range of over 3600 km with an identical battery fraction. The energy necessary to travel over a very large distance can thus be easily carried on-board with a battery percentage lower than that of most commercial full electric cars.

VIII. Charging

Suppose the on-board battery is charged only while in a station. Further assume the flux density is no higher than during the launch.[1] The optimal frequency for the fixed shore-coils with pole-pitch τ would preferably be close to the cross-over speed from constant acceleration to constant power, which is equal to $v_x = \frac{p_{\text{spec}}}{a_{\text{max}}}$ (m/s).

$$f_{\text{shorecoil}} \leq \frac{v_x}{2\tau} \quad \text{(Hz)} \tag{11}$$

With the example values in table IV, the frequency $f_{\text{shorecoil}}$ would be 334 Hz (being the lowest frequency with maximum power). At this frequency in the station at standstill the pod is able to receive the rated power of 1 MW, charging the 200 kWh battery with 5 C, well within the capacity of LiPo batteries.

IX. Example system with trains of pods

A trip of 600 km is used to illustrate the potential of the proposed system. Fig.7 shows speed, acceleration, power and energy for four different specific powers p_{spec}. Travel-time in all cases is within one hour and hardly goes down when p_{spec} goes up. The coasting power is only 3.6 kW/pass, in a cruising A380 this is 300 kW/pass (fuel power) at slighly higher speed.

As shown in table IV, when keeping a safe distance between pods (minimum distance 24.5 km), only 17 launches per hour

[1] This is a question of cost- or efficiency-optimization, see [6] for a model of core losses.

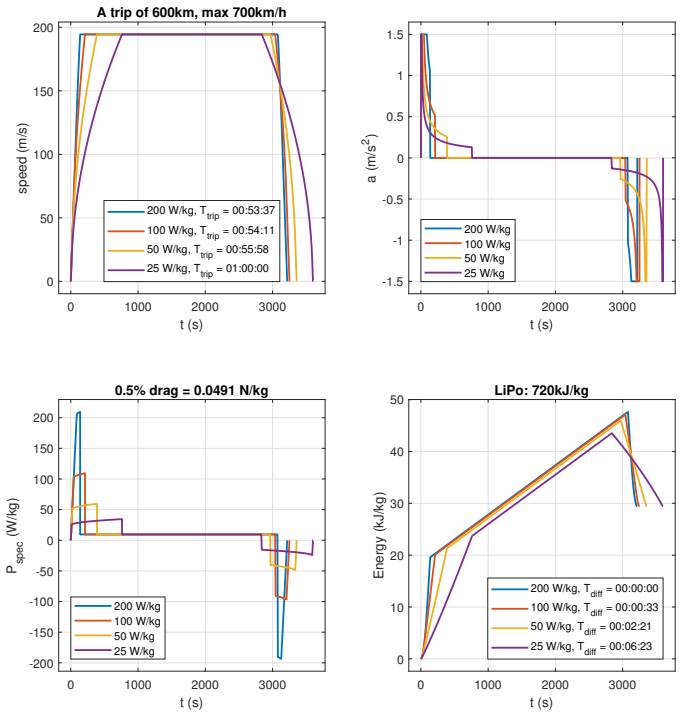

Fig. 7. Example trip of 600 km with 0.5 % drag ($C_{\text{susp}} = 0.005$).

can be made per tube. To compete with a single-track high-speed railway doing about 1000 passengers/hour, one needs 36 pods/hour with 28 pass/pod. Safe braking-distance can be met by connecting at least three pods together into a train-of-pods. Let's take a train of 5 pods, this results in 17 launches per hour; each pod propels its own share of the train-of-pods. From the values in table IV the station power can be calculated: (17×5 pod/h)×(82 kWh/trip)=7.0 MW, no sub-stations needed, doing 1.4 million passenger-kilometers per hour in a single tube (5 Wh/km/pass).

A. *Conclusions*

Compared to magnetic levitation, rolling on wheels in near vacuum achieves lowest energy use per person per distance at lowest initial cost. Operational cost need further investigation. The low drag bounds the trip-energy such that it can be buffered on-board with ease. Several thousands of kilometers of range is possible with a reasonable battery weight. An on-board motor is most effective and least expensive. A short-stator linear motor for speeding up and slowing down around the stations and a small rotating motor for coasting are suggested. The magnets and solid-back-iron remain at rest in the track, hence the pod's weight stays low. By using active stators in the stations at (fixed) frequency, fast-charging of the on-board batteries is controllable by the self-sensing field-oriented on-board inverter. Vehicle length an weight require only low tangential stress in the airgap such that current density in the Litz-wire wound pod-coil can be limited and LSM motor efficiency will be excellent. A small speed-keeper induction motor can complete the trip, fed from the battery,

TABLE IV
EXAMPLE PERFORMANCE OF ACTIVE POD ON WHEELS.

Item	value	unit
Trip distance	600	km
Cruise speed	700	km/h (194m/s)
Pod-payload	28	pass.
Pod-mass loaded	10000	kg
Kinetic energy	52	kWh (188MJ)
Travel time	0:55	hour (time while moving)
Battery-mass (LiPo)	1000	kg (10%), 200kWh
Pod-power	1000	kW (100W/kg)
Air pressure in tube	< 300	Pa
Accel distance	24.5	km
Accel time	3:32	min
Charging time	7	min (2 trains in station)
Energy per trip	82	kWh
Station power	7000	kW (on each end)
f pod	-300...970	Hz (pole-pitch $\tau = 0.1$ m)
f shore-stator	300	Hz or other constant value
LDFM length	2×150	m (2 trains in station)
LSM length	$< 2 \times 25$	km (partial LSRELM?)
IM length	551	km
wheel diameter	1	m (rough estimate)
wheel and IM speed	3700	rpm @ 700km/h
drag force	200...500	N ($C_{\text{susp}} = 0.002...0.005$)
IM torque	100...250	Nm
IM power	40...100	kW (4...10W/kg)
pod length	15	m
coil height	0.15	m
max thrust	15	kN (@ 1.5m/s^2)
max tangential stress	0.7	N/cm^2 (7 kPa)
train length	5	pods (total 140 passengers)
Launches/hour	17	Safe distance (24.5km)
flow	2380	passengers / hour
e-milage	$\approx 3..10$	Wh/km per passenger

just rails required in the largest part of the tube. Even LIM or LSRELM are possible and need further investigation.

There is no need for a huge amount of expensive shore-converters with complicated control as is the case in long-stator designs. No need for long active tracks, high acceleration, magnetic levitation nor super-conductors. Excellent efficiency and economy seems feasible without all that.

REFERENCES

[1] S. Zhu, Y. Cai, R.M. Rote and S.S. Chen, "Magnetic damping for maglev", Shock and Vibration 5 (1998) 119128.

[2] A. Cassat and M. Jufer, "MAGLEV Projects Technology Aspects and Choices" IEEE Transactions on Applied Superconductivity 12(1):915-925, April 2002.

[3] Michael Flankl, Tobias Wellerdieck, Arda Tysz and Johann W. Kolar, "Scaling laws for electrodynamic suspension in high-speed transportation", IET Research Jounals, pp. 1-8. 2015.

[4] (https://hyperloop-one.com/blog/... how-and-why-were-levitating)

[5] E. Fritz, J. Klhspies, R. Kircher, M. Witt, L. Blow, "Energy Consumption of Track-Based High-Speed Trains: Maglev Systems in Comparison With Wheel-Rail Systems", Transportation Systems and Technology. 2018;4(3 suppl. 1): 134-155.

[6] Yicheng Chen, Pragasen Pillay, "An Improved Formula for Lamination Core Loss Calculations in Machines Operating with High Frequency and High Flux Density Excitation", Conference Record of the 2002 IEEE Industry Applications Conference. 37th IAS Annual Meeting.

[7] Veltman, A., Hulst, van der P., Jonker, M.C.P., Gurp, van J.P., "Sensorless control of a 2.4MW linear motor for launching roller-coasters",10th European Conference on Power Electronics and Applications, Toulouse (EPE 2003).